Analyst

Accepted Manuscript

ROYAL SOCIETY OF CHEMISTRY

www.rsc.org/analyst

Cite this: DOI: 10.1039/c0xx00000x

www.rsc.org/xxxxxx

ARTICLE TYPE

In situ synthesis of metal-organic frameworks in porous polymer monolith as stationary phase for capillary liquid chromatography

Shengchao Yang, Fanggui Ye,* Cong Zhang, Shufen Shen and Shulin Zhao

Received (in XXX, XXX) Xth XXXXXXXXX 20XX, Accepted Xth XXXXXXXXX 20XX

DOI: 10.1039/b000000x

In this study, HKUST-1 was synthesized in situ on the porous polymer monolith as stationary phase for capillary liquid chromatography (cLC). The unique carboxyl functionalized poly(methacrylic acid-co-ethylene dimethacrylate) (poly(MAA-co-EDMA)) monolith was used as a support to directly grow HKUST-1 by a controlled layer-by-layer self-assembly strategy. X-ray diffraction, scanning electron microscopy, energy dispersive X-ray spectrometry, and Fourier transform infrared spectroscopy of the resulting HKUST-1-poly(MAA-co-EDMA) monoliths indicated that HKUST-1 was successfully grafted onto the pore surface of the poly(MAA-co-EDMA) monolith. The column performance of HKUST-1-poly(MAA-co-EDMA) monoliths for the separation of various small molecules, such as benzenediols, xylenes, ethylbenzene, and styrene, was evaluated. The chromatographic performance was found to improve with increasing HKUST-1 density, and the column efficiencies and resolutions of HKUST-1-poly(MAA-co-EDMA) monolith were 18,320–19,890 plates/m and 1.62–6.42, respectively, for benzenediols. The HKUST-1-poly(MAA-co-EDMA) monolith displayed enhanced resolution for the separation of positional isomers when compared to the traditional C18 and HKUST-1 incorporation polymer monoliths. Hydrophobic, π–π, and hydrogen bonding interactions within the HKUST-1-poly(MAA-co-EDMA) monolith were observed in the separation of small molecules. The results showed that the HKUST-1-poly(MAA-co-EDMA) monoliths are promising stationary phases for cLC.

1. Introduction

Metal-organic frameworks (MOFs) are composed of metal ions or clusters, and coordinating linkers that impart high porosity and crystallinity to their structures.[1] In recent times, MOFs have attracted considerable attention in various fields, including gas storage,[2] energy storage, [3] catalysis,[4]drug delivery,[5] sensing,[6] and separation,[7] due to their diverse structures and fascinating properties, such as exceptionally large surface area, highly uniform pores, and tunable pore geometry[8]. These unique properties and wide structural choices also make MOFs attractive candidates for stationary phases in solid-phase extraction[9] and chromatography,[10,11] specifically for packed columns and coated capillary columns in high resolution gas chromatography (GC).[12] Recently, various MOFs (particles/powders of MIL-101, MIL-53, MIL-100, HKUST-1, MOF-5 and MIL-47) have been ground or directly packed into columns as the stationary phase for high performance liquid chromatography (HPLC).[13-18] However, MOFs particles often suffer from widely distributed sizes and irregular shapes, which could result in low column efficiency, high column backpressure, and undesirable peak shapes.

MOF composites exhibit new properties that are superior to those of the individual components through the collective behavior of the functional units[19]. MOF-based composite is a rapidly developing interdisciplinary research area, which represents a new material with specific functional properties and.[20-22] The synthesis of MOFs-based composites, such as MOFs/silica and MOFs/organic polymers is an effective strategy to overcome the above-mentioned problems. In attempts to combine the good column packing properties of a spherical substrate, and the unique separation ability of MOFs, MOFs/silica composites have been explored as stationary phases in HPLC.[23-26] MOFs/organic polymer hybrids, which combine the advantages of MOFs and polymer monoliths, are attractive for improving the separation performance of MOFs materials in HPLC. Various microsized MOFs, such as MIL-101(Cr)[27] and UIO-66[28] were incorporated into polymer monoliths for capillary electrochromatography (CEC), and HPLC separation of small molecules, resulting in enhanced resolution and high column efficiency. In our previous work, HKUST-1 nanoparticles were incorporated into polymer monoliths to afford stationary phases with the enhanced chromatographic performance for the separation of small molecules.[29] It was observed that increasing the amount of HKUST-1 nanoparticles in the polymerization mixture improved the separation and column efficiency. However, upon further increase of the amount of HKUST-1 nanoparticles, the monoliths exhibited serious non-uniformity, and a portion of the nanoparticles sank to the bottom of the column. This was attributed to the high surface energy and large van der Waals forces, which resulted in the aggregation of HKUST-1 nanoparticles. The poor dispersion of the microsized

MOFs in the polymer matrix is a significant drawback for fully displaying their excellent separation capabilities. Moreover, the low external surface area to volume ratio of the MOFs crystals, and the large distance between the crystal surface and the majority of the pore volume, can cause slow diffusion into the pore structure, relative to diffusion through the polymer monolith.[30] Recently, Bao et al.[31] developed HKUST-1-grown capillary column by using liquid-phase epitaxy process for open-tubular CEC and capillary liquid chromatography(cLC). However, open-tubular capillary column is not popular due to low sample loadability and the relatively smaller inner diameter of capillary. Therefore, the development of a simple approach for the incorporation of high content of dispersed MOFs into a polymer monolith, where the majority of the pores are close to the surface, is highly desirable.

HKUST-1, which is one of the most widely investigated MOFs, in theory and experiment, is assembled from Cu^{2+} cations and benzene-1,3,5-tricarboxylate (H_3BTC) linker molecules, which have a paddle-wheel structure.[32] In this study, HKUST-1 is used as a model MOFs to demonstrate the in situ layer-by-layer self-assembly method to graft MOFs on the surface of poly(methacrylic acid-co-ethylene dimethacrylate) (poly(MAA-co-EDMA)) monolith. To the best of our knowledge, studies on the development of in situ synthesized MOFs in porous polymer monolith, as stationary phase for HPLC have been not reported. The resulting HKUST-1-poly(MAA-co-EDMA) monolith was evaluated and proposed as the stationary phase for reversed phase capillary liquid chromatography (RP-cLC). The chromatographic performance of the HKUST-1-poly(MAA-co-EDMA) monolith was tested with a variety of benzenediols, xylenes, ethylbenzene, and styrene.

2. Experimental

2.1 Reagents and materials

Methacrylic acid (MAA), ethylene dimethacrylate (EDMA), octadecyl methacrylate (OMA), cyclohexanol and 3-(trimethoxysilyl)propyl methacrylate (γ-MAPS) were purchased from Alfa Aesar (Ward Hill, MA, USA). Azobisisobutyronitrile (AIBN) was obtained from Tianjin Chemistry Reagent Factory (Tianjin, China) and recrystallized in ethanol prior to use. Benzene, toluene, ethylbenzene, n-propylbenzene, n-butylbenzene and styrene were purchased from TCI (Shanghai, China). The xylenes, m-benzenediol, o-benzenediol, p-benzenediol, $Cu(Ac)_2$, 1,3,5-benzenetricarboxylic acid (H_3BTC), ethanol, HPLC-grade methanol, and acetonitrile were obtained from Shanghai Chemical Reagents Corporation (Shanghai, China). All reagents were of analytical grade or better. Ultrapure water obtained from a Milli-Q water system (Millipore, Bedford, MA, USA) was used in all experiments. Fused-silica capillaries (100 μm i.d. × 375 μm o.d.) were obtained from Reafine Chromatography Ltd (Hebei, China).

2.2 Instrumentation

All chromatographic experiments were performed on a TriSep-2100 pressurized capillary electrochromatography system (this instrument could also be utilized as a capillary liquid chromatography (cLC) system; Unimicro Technologies, Pleasanton, CA, USA) equipped with a UV detector. The flow rate was 0.05 mL/min, the UV absorbance was monitored at 214 nm, and the supplement pressure was 1000 psi, unless otherwise stated. Monolithic columns with a total length of 36 cm (effective length 26 cm) were used unless otherwise stated. Fourier transform infrared (FT-IR) spectra (4000–400 cm^{-1}) in KBr were recorded using a PE Spectrum One FT-IR spectrometer (PE, USA). Powder X-ray diffraction (XRD) patterns were recorded on a D/max 2550 VB/PC diffractometer (Rigaku, Japan) with Cu Kα radiation (λ = 0.15418 nm). Scanning electron microscopy (SEM) and energy dispersive X-ray spectrometry (EDS) experiments were carried out on an FEI Quanta 200 FEG SEM (Philips, The Netherlands). To overcome charging issues, samples of the prepared monoliths were sputter coated with gold, prior to SEM. Micromeritics ASAP 2020M (Micromeritics, USA) were used to determine the Brunauer-Emmett-Teller (BET) surface areas of monoliths.

2.3 Preparation of HKUST-1-poly(MAA-co-EDMA) monolith

The vinylized capillary was prepared as following: a 50% γ-MAPS methanol (v/v) solution was used to introduce the vinyl groups onto the inner surface of capillary according to a previously described procedure.[33] The bare poly(MAA-co-EDMA) monolith was prepared from polymerization mixtures consisting of MAA (20 μL), EDMA (200 μL) and cyclohexanol (1200 μL), using AIBN (4.5 mg) as an initiator. The polymerization mixtures were sonicated for 10 min to obtain clear solutions, followed by manual injection of the mixture into the vinylized capillary to an appropriate length with a 1 mL syringe. Both ends of the capillary were then sealed with pieces of rubbers, and the capillary was submerged in a water bath at 60°C for 16 h. The monolithic columns thus obtained, were flushed with methanol to remove residual monomers and porogens.

At room temperature, a 10 mM solution of $Cu(Ac)_2$ in ethanol was pumped through the bare poly(MAA-co-EDMA) monolith for 15 min. After rinsing with ethanol for 5 min, the Cu^{2+} modified monolith was reacted with an ethanolic solution of H_3BTC (10 mM) for 30 min. This resulted in one layer of HKUST-1 coated on the surface of the poly(MAA-co-EDMA) monolith by coordinate bonds. After a given number of cycles of

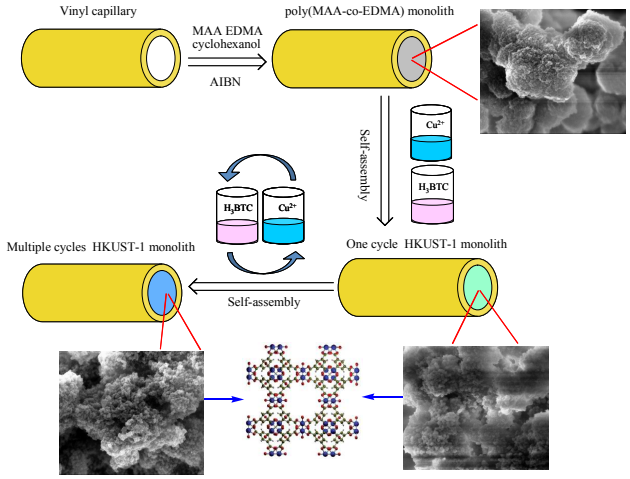

Fig.1 Scheme Schematic diagram for the synthesis of HKUST-1-poly(MAA-co-EDMA) monoliths

alternately pumping with ethanolic solutions of $Cu(Ac)_2$ and H_3BTC, a series of HKUST-1-poly(MAA-co-EDMA) monoliths were successfully synthesized. These were counterbalanced with methanol for 3 h and filled with methanol for storage until use. The general scheme for synthesis of HKUST-1-poly(MAA-co-EDMA) monolith is shown in Fig. 1. During the entire chemical modification process, a pumping flow of 0.1 mL/min was applied across the monolithic columns. A detection window was created 2 mm after the end of the polymer bed, using a thermal wire stripper, and a 2 cm length of the capillary containing the monolith was cut for SEM and EDS analysis. The bare poly(MAA-co-EDMA) and HKUST-1-poly(MAA-co-EDMA) materials were also prepared in a 5 mL centrifuge tube, washed with methanol, and dried overnight at 150 °C for XRD and, FT-IR studies. For comparison, C18 polymer monoliths were prepared from polymerization mixtures consisting of OMA (0.54 g), EDMA (0.36 g), 1,4-butanediol (0.63 g), cyclohexanol (1.47 g), and AIBN (9 mg) by procedure described above. The bulk poly(MAA-co-EDMA) and HKUST-1-poly(MAA-co-EDMA) materials were also prepared according to a previously described procedure[30] for FT-IR, XRD, EDS and N_2 sorption isotherm characterization.

2.4 Calculations

The permeability (K) was calculated by the following formula described in our previous work [29]

$$K = \frac{F \times \eta \times L}{\Delta P \times \pi \times r^2}$$

where F is the volume flow rate of the eluent, η is the dynamic viscosity of the mobile phase, L is the column length, and ΔP is the pressure drop across the column. In this work, methanol was used as mobile phase and corresponding value of dynamic viscosity was 0.580×10^{-3} kg/(m×s) at 25 ℃.

3. Results and discussions

3.1 Characterization of the HKUST-1-poly(MAA-co-EDMA) monolith

The synthesized HKUST-1-poly(MAA-co-EDMA) monoliths were characterized by SEM, XRD, FT-IR and SEM-EDS. A comparison of the SEM images (Fig. 2A and B), shows the numerous octahedral HKUST-1 nanoparticles attached to the surface of the poly(MAA-co-EDMA) monolith, confirming that HKUST-1 was synthesized successfully onto the pore surface of the poly(MAA-co-EDMA) monolith. The structures of the resulting HKUST-1-poly(MAA-co-EDMA) monoliths with 0, 2, 4, 6 cycles (named as 0-LC, 2-LC, 4-LC and 6-LC monoliths) were obtained from the XRD pattern (Fig. 2C). While the XRD pattern is dominated by the amorphous polymer monolithic matrix (very broad signal at $2\theta \approx 40°$), HKUST-1 nanoparticles in the HKUST-1-poly(MAA-co-EDMA) monolith were confirmed by their characteristic peaks. The characteristic stretching vibrations of the aromatic C=C (1606 cm^{-1}) and C-H (730-790 cm^{-1}) bonds of HKUST-1 and C-H bond (2960 cm^{-1}) of poly(MAA-co-EDMA) were observed in the FT-IR spectra of the HKUST-1-poly(MAA-co-EDMA) monolith (Fig. 2D), which further confirmed that the HKUST-1 was grafted onto the poly(MAA-co-EDMA) monolith. The HKUST-1-poly(MAA-co-EDMA) monoliths obtained by controlled fabrication were characterized by analysis of their SEM images and EDS spectra.

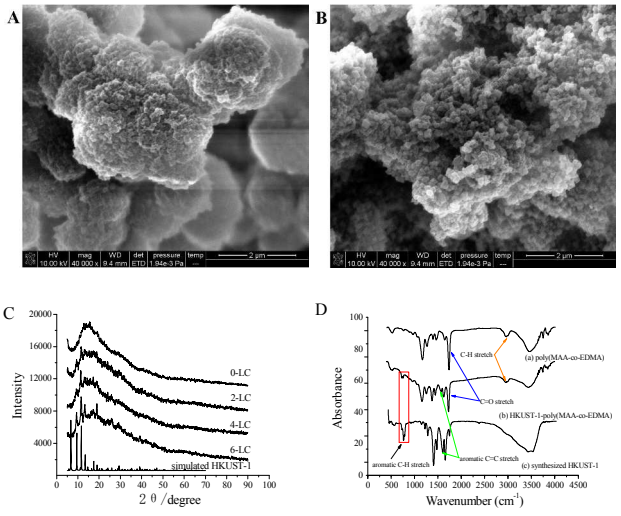

Fig.2 SEM images of (A) poly(MAA-co-EDMA) and (B) HKUST-1-poly(MAA-co-EDMA) monoliths. (C) XRD patterns of the synthesized HKUST-1-poly(MAA-co-EDMA) monoliths, and HKUST-1 (simulated) and. (D) FT-IR spectra of synthesized poly(MAA-co-EDMA) monolith, HKUST-1-poly(MAA-co-EDMA) monolith and HKUST-1.

Table 1 Effect of self-assembly cycles on the backpressure and permeability of monoliths

Column	Monomers		Porogens	HKUST-1 (LC)	Back pressure (MPa)	Permeability ($\times10^{-14}$ m^2)	BET suface area (m^2/g)
	MAA (μL)	EDMA (μL)	Cyclohexanol (μL)				
a	20	200	1200	0	4.8	8.72	95
b	20	200	1200	2	7.6	5.51	145
c	20	200	1200	4	16.1	2.60	197
d	20	200	1200	6	18.3	2.23	261
e	20	200	1200	8	>25.0	---	---

[a] Backpressure is obtained with methanol as the mobile phase at 5 μL/min without splitting flow.

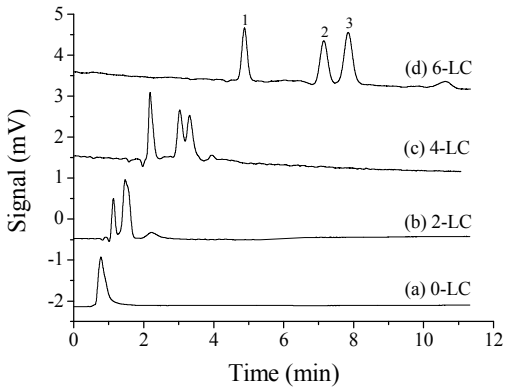

Fig.3 Chromatograms of benzenediols on 0-LC, 2-LC, 4-LC and 6-LC monoliths. Conditions: mobile phase, acetonitrile/H_2O (40/60, v/v); flow rate, 0.05 mL/min; UV detection at 214 nm; supplement pressure, 1000 psi. Solutes 1, *p*-benzenediol; 2, *m*-benzenediol; 3, *o*-benzenediol.

The SEM images revealed a uniform monolithic matrix with octahedral HKUST-1 nanoparticles and large through-pores (Fig. S1e, h and k). From the EDS results, it was seen that the Cu was not detected in the bare poly(MAA-co-EDMA) monolith (Fig. S.1c). In contrast, the 2-LC monolith contained Cu (17.77%, w/w), which increased to 31.52% (w/w) in the 6-LC monolith, showing that the density of HKUST-1 increased with increasing number of assembly cycles. The HKUST-1 incorporation monolith contained 3.21% (Cu, w/w),[29] indicating that the in situ layer-by-layer self-assembly method was an effectively strategy to increase the content of HKUST-1 nanoparticles in the porous polymer monoliths. The permeability of the as-prepared monoliths decreased with increasing number of assembly cycles (Table 1). N_2 sorption isotherm was presented in Fig. S2. The increased BET surface areas of the HKUST-1-poly(MAA-co-EDMA) monoliths (145 m^2/g for 2-LC, 197 m^2/g for 4-LC and 251 m^2/g for 6-LC) as compared to the bare poly(MAA-co-EDMA) monolith (101 m^2/g) also imply the effective loading of HKUST-1 on the surface of poly(MAA-co-EDMA) monoliths.

The influence of pH on the chemical stability of HKUST-1 was investigated by dispersing HKUST-1 nanoparticles in buffers with different pH at room temperature for 24 h. The XRD patterns of the resultant samples retained peaks belonging to HKUST-1, implying the stability of HKUST-1 in the pH ranges of 4–11.6 (Fig. S3).

3.2 Effect of HKUST-1 density on cLC separation

In order to study the effect of HKUST-1 density on cLC performance, the separation of benzenediols on HKUST-1-poly(MAA-co-EDMA) monoliths with different number of assembly cycles was investigated (Fig. 3). All the benzenediols were eluted as an overlapped peak on the bare poly(MAA-co-EDMA) monolith due to its low BET surface area (Fig. 3a). However, the column efficiency and resolution of benzenediols improved greatly with the increasing number of assembly cycles, which was attributed to an increase in the density of HKUST-1 of the HKUST-1-poly(MAA-co-EDMA) monoliths. For example, the column efficiencies and resolutions of 6-LC monoliths were 18,320–19,890 plates/m and 1.62–6.42 for benzenediols, respectively, which were only 5,500–10,700 plates/m and 0.85–3.57 on the 4-LC monolith under the same experimental conditions (Table 2). The Van Deemter plot of *p*-benzenediol was showed in Fig. S4. The minimum plate heights of 50.7 μm was achieved for *p*-benzenediol, which corresponds to the column efficiency of 19,720 plates/m.Thus, the density of HKUST-1 in the prepared monoliths played a significant role in the enhanced separation of benzenediols by cLC, and a baseline

Table 2 Effect of number of self-assembly cycles on the performance of HKUST-1-poly(MAA-co-EDMA) monoliths. Data were calculated from Fig. 3.

Column	Parameters	*p*-Benzenediol	*m*-Benzenediol	*o*-Benzenediol
6- LC	t_R(min)	4.888	7.154	7.854
	R_s	…	6.42	1.62
	N(plates/m)	18,320	19,890	19,710
4 -LC	t_R(min)	2.195	3.042	3.326
	R_s	…	3.57	0.85
	N(plates/m)	5,500	11,060	10,660
2- LC	t_R(min)	1.146	1.483	1.483
	R_s	…	1.32	…
	N(plates/m)	3,060	…	…
0 -LC	t_R(min)	0.783	0.783	0.783
	R_s		overlap	
	N(plates/m)		overlap	

[a] Footnote text.

separation was achieved on the 6-LC monolith (Fig. 3d). However, further increase of the number of assembly cycles resulted in a high backpressure (>25.0 MPa, Table 1). Based on the above results, the 6-LC monolith was used in all further experiments.

3.3 Chromatographic performance

3.3.1 Separation of positional isomers

Although selective separation of positional isomers is of great importance in industry, their similar physical and chemical properties cause difficulties. In this work, we studied benzenediols, xylenes, and ethylbenzene isomers to evaluate the advantages of HKUST-1-poly(MAA-co-EDMA) monolith for fast and efficient separation of positional isomers.

Benzenediol isomers were used to investigate the characteristics of the HKUST-1-poly(MAA-co-EDMA) monolith for RP-cLC. The retention values of the benzenediols decreased with increasing acetonitrile content in the mobile phase (Fig. S5), which showed the RP characteristic of the HKUST-1-poly(MAA-co-EDMA) monolith. A comparison of the chromatographic performance of the HKUST-1-poly(MAA-co-EDMA) and C18 polymer monoliths (Fig. 4) showed that the retentions of benzenediols were weak on the C18 polymer monolith, resulting in fast elution and poor resolutions, while the HKUST-1-poly(MAA-co-EDMA) monolith showed a baseline separation of the benzenediols under the same experimental conditions. The separation of benzenediol isomers on the HKUST-1-poly(MAA-co-EDMA) monolith was ascribed to the hydrogen bonding interaction between the carboxyl ligand in HKUST-1 framework

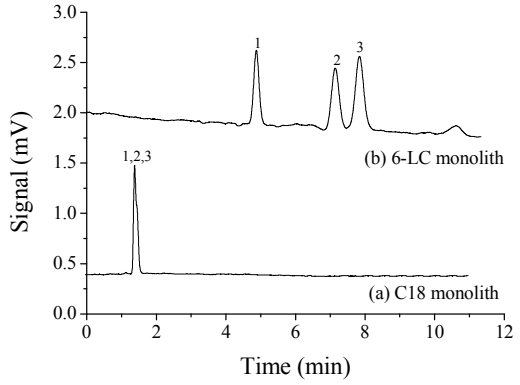

Fig.4 Chromatograms of benzenediols on C18 and 6-LC monoliths Conditions: mobile phase, acetonitrile/H_2O (40/60, v/v). Other conditions are same as in Fig. 3. Solutes 1, *p*-benzenediol; 2, *m*-benzenediol; 3, *o*-benzenediol.

and benzenediol isomers, which is similar to the results reported for MIL-53(Al).[16] The elution sequence of benzenediols on the HKUST-1-poly(MAA-co-EDMA) monolith was *p*- < *m*- < *o*-isomer, which is consistent with the increase in acidity from *p*-benzenediol (pKa 9.91) to *m*-benzenediol (pKa 9.30) and to *o*-benzenediol (pKa 9.28).[34] As *p*-benzenediol is the weakest proton donor among the three isomers, it has the weakest hydrogen bonding interactions with the carboxyl ligand in HKUST-1, leading to it being eluted first. The separation performance of the HKUST-1-poly(MAA-co-EDMA) monolith was also compared to HKUST-1 incorporated monolith [29] (Fig. 5) and found to yield a higher resolution. This was attributed to the higher density of HKUST-1 in the former, which allows for stronger interaction between the analytes and monolithic stationary phase. Compared with the previous report,[16] where the baseline separation of benzenediols was accomplished in about 60 min on the MIL-53(Al) packed column in RP mode, the HKUST-1-poly(MAA-co-EDMA) monolith exhibited a faster and more efficient separation (9 min).

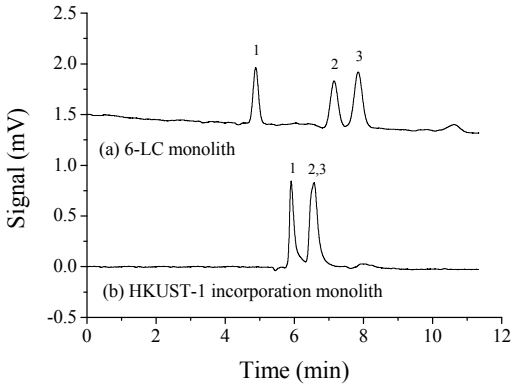

Fig.5 Chromatograms of benzenediols on HKUST-1 incorporation and 6-LC monoliths. Conditions: mobile phase, acetonitrile/H_2O (40/60, v/v). Other conditions are same as in Fig. 3. Solutes 1, *p*-benzenediol; 2, *m*-benzenediol; 3, *o*-benzenediol.

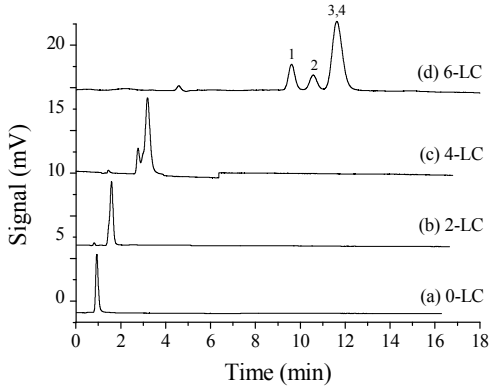

Fig.6 Chromatograms of the ethylbenzene and xylenes on 0-LC, 2-LC, 4-LC and 6-LC monoliths. Conditions: mobile phase, acetonitrile/H_2O (60/40, v/v). Other conditions are same as in Fig. 3. Solutes 1, ethylbenzene; 2, *p*-xylene; 3, *m*-xylene; 4, *o*-xylene.

To further evaluate the chromatographic performance of the HKUST-1-poly(MAA-co-EDMA) monolith in the separation of positional isomers, xylenes and ethylbenzene were used as test analytes. Investigation of HKUST-1-poly(MAA-co-EDMA) monolith for RP chromatography provided a partial separation of the ethylbenzene and xylene isomers using a binary polar mobile phase (acetonitrile/H_2O) (Fig. 6). The retention and elution order of these positional isomers are ethylbenzene < *p*-xylene < *o*-and *m*-xylenes, which indicates the fact that HKUST-1 exhibits higher affinity for bulkier molecules with higher kinetic diameter and lower van der Waals volume.[35] HKUST-1 possesses a three

dimensional framework with a paddle-wheel structure featuring pores with different sizes and shapes, which are large square-shaped pores of diameter ~9 Å.[32] The critical kinetic diameters of ethylbenzene, *p*-xylene, *m*-xylene and *o*-xylene are 6.7, 6.7, 7.1 and 7.4 Å, respectively; and their van der Waals volumes are

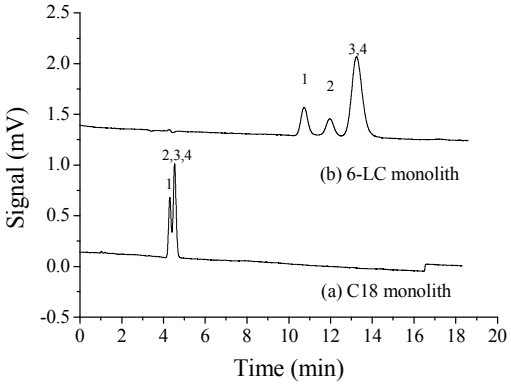

Fig.7 Chromatograms of ethylbenzene and xylenes on C18 and 6-LC monoliths. Conditions: mobile phase, acetonitrile /H_2O (55/45, v/v). Other conditions are same as in Fig. 3. Solutes 1, ethylbenzene; 2, *p*-xylene; 3, *m*-xylene; 4, *o*-xylene.

120.20, 120.13, 120.04 and 119.91 nm3, respectively.[36] The stronger retentions of *o*-and *m*-xylene were attributed to higher kinetic diameters, which resulted in increased effective contact with the pores of HKUST-1. Moreover, decreased retention of the test analytes was observed with increasing acetonitrile content in the mobile phase, which exhibited an RP retention mechanism for all isomeric analytes (Fig. S6). The separation of ethylbenzene and xylene isomers with the same mobile phase on HKUST-1-poly(MAA-co-EDMA), C18, and HKUST-1 incorporation monoliths were compared. It was seen that the HKUST-1-poly(MAA-co-EDMA) monolith yielded a higher resolution for the positional isomers in RP mode than the C18 monolith (Fig. 7), and the HKUST-1 incorporated monolith (Fig. 8).

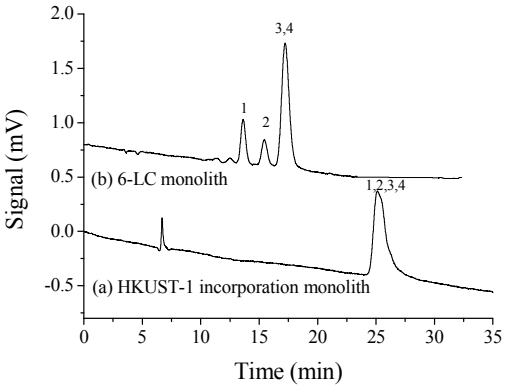

Fig.8 Chromatograms of ethylbenzene and xylenes on HKUST-1 incorporation monolith and 6-LC monoliths. Conditions: mobile phase, acetonitrile/H_2O (50/50, v/v). Other conditions are same as in Fig. 3. Solutes 1, ethylbenzene; 2, *p*-xylene; 3, *m*-xylene; 4, *o*-xylene.

The above results clearly indicated that the HKUST-1-poly(MAA-co-EDMA) monolith is an effective alternative to traditional nonpolar columns for the separation of positional isomers in the RP mode.

3.3.2 Separation of ethylbenzene and styrene

Ethylbenzene and styrene are of significant industrial importance and usually produced as mixtures but difficult to separate by the standard distillation method due to their similar boiling points. Although the baseline separation of ethylbenzene and styrene could be achieved on MOF-based columns for HPLC in the previous reports, these studies were performed in normal phase mode with a nonpolar organic solvent as the mobile phase.[13,23,25,26] The separation of ethylbenzene and styrene was realized with a good resolution by the HKUST-1-poly(MAA-co-EDMA) monolith using a binary polar mobile phase (acetonitrile/H_2O) (Fig. 9). The retention of ethylbenzene and styrene, and their resolutions, increased with increasing number of assembly cycles (Fig. 9), showing that increasing the HKUST-1 density improved the separation efficiency. Moreover, the retention values of ethylbenzene and styrene decreased with increasing acetonitrile content in the mobile phase (Fig. S7). It is likely that the π–π interactions (between the aromatic analytes and the BTC ligand in HKUST-1), and the interaction between π electrons and the potentially uncoordinated Cu^{2+} ligation sites, led to the separation of ethylbenzene and styrene in the previous reports.[13,23,25] However, the unsaturated Cu^{2+} sites of HKUST-1 preferred to coordinate to H_2O molecules when acetonitrile/H_2O was used as the mobile phase. Therefore, the π–π interaction was believed to be responsible for the separation of ethylbenzene and styrene in the present case, where styrene has a stronger interaction with HKUST-1, resulting in a longer elution time. Upon comparison with the C18 monolith, the HKUST-1-poly(MAA-co-EDMA) monolith gave the contrary elution order of ethylbenzene and styrene (Fig. S8), also indicating that the retention mechanism was based on the π–π interactions.

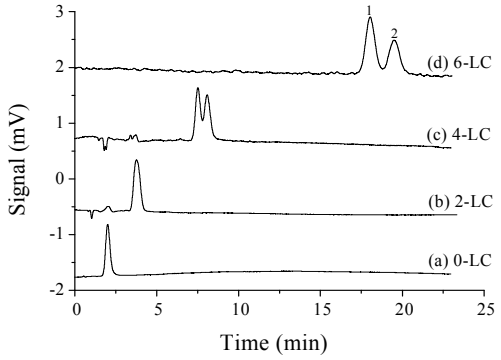

Fig.9 Caption Chromatograms of ethylbenzene and styrene on 0-LC, 2-LC, 4-LC and 6-LC monoliths. Conditions: mobile phase, acetonitrile/H_2O (45/55, v/v). Other conditions are same as in Fig. 3. Solutes 1, ethylbenzene; 2, styrene.

3.4 Reproducibility and stability

The reproducibility and stability properties of the 6-LC monolith were evaluated in terms of the retention times of benzenediols. The relative standard deviations (RSDs) for the retention time of analytes were less than 1.6% (n=6) and 2.8% (n=5) for run-to-run, day-to-day, respectively. Column-to-column reproducibility

was also investigated with three batches of the 6-LC monolith. The RSD of the migration time of the analytes was less than 8.2% (n=3). Moreover, the 6-LC monolith demonstrated a good running stability and could be used for more than 200 runs without obvious changes in the separation efficiency. The above results indicated that the prepared HKUST-1-poly(MAA-co-EDMA) monolith have good reproducibilities and stability.

4. Conclusions

In conclusion, HKUST-1-poly(MAA-co-EDMA) monolith was fabricated successfully by an in situ layer-by-layer self-assembly method, where the HKUST-1 was grafted onto the surface of poly(MAA-co-EDMA) monolith. The HKUST-1-poly(MAA-co-EDMA) monolith was explored for separation of small molecules in RP mode with high resolution and good selectivity. These successful separations suggest that the proposed monoliths have great potential for HPLC separation based on the combined mechanisms of hydrophobic, π–π and hydrogen bonding interactions compared to the traditional C18 columns.

Acknowledgements

The financial support from the National Natural Science Foundation of China (No. 21365005), Guangxi Natural Science Foundation of China (2012GXNSFAA053024 and 2014GXNSFGA118002) are gratefully acknowledged.

Notes and references

Key Laboratory for the Chemistry and Molecular Engineering of Medicinal Resources (Ministry of Education of China), College of Chemistry and Pharmaceutical Science of Guangxi Normal University, Guilin 541004, P. R. China.
Corresponding author: Prof. Fanggui Ye
Tel: +86-773-5856104; fax: +86-773-5832294
E-mail address: *fangguiye@163.com*

1. H. Furukawa, K. E. Cordova, M. O'Keeffe and O. M. Yaghi, Science, 2013, 341, 974-986.
2. P. M. Suh, H. J. Park, T. K. Prasad and D. W. Lim, Chem Rev, 2011, 112, 782-835.
3. J.-K. Sun and Q. Xu, Energy Environ Sci, 2014, 7, 2071-2100.
4. J. Y. Lee, O. K. Farha, J. Roberts, K. A. Scheidt, S. T. Nguyen and J. T. Hupp, Chem Soc Rev, 2009, 38, 1450-1459.
5. P. Horcajada, R. Gref, T. Baati, P. K. Allan, G. Maurin, P. Couvreur, G. Férey, R.E. Morris and C. Serre, Chem Rev, 2012, 112, 1232-1268.
6. J. Lei, R. Qian, P. Ling, L. Cui and H. Ju, Trends Anal Chem, 2014, 58, 71-78
7. J. -R. Li, J. Sculley and H. -C. Zhou, Chem Rev, 2012, 112, 869-932.
8. M. Li, D. Li, M. O'Keeffe and O. M. Yaghi, 2014, 114, 1343-1370.
9. Y. Hu, Z. Huang , J. Liao and G. Li, Anal Chem, 2013, 85, 6885-6893.
10. Y. Yu, Y. Ren, W. Shen, H. Deng and Z. Gao, Trends Anal Chem, 2013, 50, 33-41.
11. Z.-Y. Gu, C.-X. Yang, N. Chang and X.-P. Yan, Acc Chem Res, 2012, 45, 734-745.
12. K. Yusuf, A Aqel and Z. ALOthman, J Chromatogr A, 2014, 1348, 1-16.
13. R. Ahmad, A. G. Wong-Foy and A. J. Matzger, Langmuir, 2009, 25 11977-11979.
14. L. Alaerts, C. E. A. Kirschhock, M. Maes, M. A. van der Veen, V. Finsy, A. Depla, J. A. Martens, G. V. Baron, P. A. Jacobs, J. F. M. Denayer and D. E. De Vos, Angew Chem Int Ed, 2007, 46, 4293-4297.
15. L. Alaerts, M. Maes, L. Giebeler, P. A. Jacobs, J. A. Martens, J. F. M. Denayer, C. E. A. Kirschhock and D. E. De Vos, J Am Chem Soc, 2008, 130, 14170-14178.
16. S.-S. Liu, C.-X. Yang, S.-W. Wang and X.-P. Yan, Analyst, 2012, 137, 816-818.
17. C. -X. Yang and X. -P. Yan, Anal Chem, 2011, 83, 7144-7150.
18. Y. -Y. Fu, C. -X. Yang and X. -P. Yan, J Chromatogr A, 2013, 1274, 137-144.
19. Q.-L. Zhu and Q. Xu, Chem Soc Rev, 2014, 43, 5468-5512.
20. A. J. Brown, N. A. Brunelli, K. Eum, F. Rashidi, J. R. Johnson, W. J. Koros, C. W. Jones and S. Nair, Science, 2014, 345, 72-75.
21. C. M. Doherty, D. Buso, A. J. Hill, S. Furukawa, S. Kitagawa and P. Falcaro, Acc Chem Res 2014, 47, 396-405.
22. J. Yao and H. Wang, Chem Soc Rev, 2014, 43, 4470-4493.
23. R. Ameloot, A. Liekens, L. Alaerts, M. Maes, A. Galarneau, B. Coq, G. Desmet, B. F. Sels, J. F. M. Denayer and D. E. De Vos, Eur J Inorg Chem, 2010, 2010, 3735-3738.
24. K. Tanaka, T. Muraoka, D. Hirayama and A. Ohnish, Chem Commun, 2012, 48, 8577-8579.
25. A. Ahmed, M. Forster, R. Clowes, D. Bradshaw, P. Myers and H. Zhang, J Mater Chem A, 2013, 1, 3276-3286.
26. Y.-Y. Fu, C.-X. Yang and X.-P. Yan, Chem Eur J, 2013, 19, 13484-13491.
27. H.-Y. Huang, C.-L. Lin, C.-Y. Wu, Y.-J. Cheng and C.-H. Lin, Anal Chim Acta, 2013, 779, 96-103.
28. Y.-Y. Fu, C.-X. Yang and X.-P. Yan, Chem Commun, 2013, 49, 7162-7164.
29. S. Yang, F. Ye., Q. Lv, C. Zhang, S. Shen and S. Zhao, J Chromatogr A, 2014, 1360, 143-149.
30. A. Saeed, F. Maya, D. J. Xiao, M. Najam-ul-Haq, F. Svec and D. K. Britt, Adv Funct Mater, 2014, 24, 5790-5797.
31. T. Bao., J. Zhang, W. Zhang and Z. Chen, J Chromatogr A, 2015, 1381, 239-246.
32. S. S.-Y. Chui, S. M. -F. Lo, J. P. H. Charmant, A. G. Orpen and I. D. Williams, Science, 1999, 283, 1148-1150.
33. R. Wu, H. Zou and M. Ye, Anal Chem 2001, 73, 4918-4923.
34. K. Hu, K. Qu, Y. Li, C. Ding, X. Wang, J. Zhang, B. Ye and S. Zhang, J Sep Sci, 2008, 31, 2430-2433.
35. Z. Yan, J. Zheng, J. Chen, P. Tong, M. Lu, Z. Lin and L. Zhang, J Chromatogr A, 2014, 1366, 45-53.
36. P. S. Bárcia, D. Guimarães, P. A. Mendes, J. A. Silva, V. Guillerm, H. Chevreau, C. Serre and A. E. Rodrigues, Microporous Mesoporous Mater, 2011, 139, 67-73.